and acceptors are utilized in the structure. (2) The columnar stacking of twofold screw-related complexes is along the *c* axis. The stacking in these columns has been discussed in detail above.

**Acknowledgment.** This investigation was supported by the donors of the Petroleum Research Fund, administered by the American Chemical Society, and by the National Institutes of Health (Biomedical Sciences Support Grant and Public Health Service Research Grant No. GM 20544).

**Registry No.** $Cu(O_3N_6C_{17}H_{20})\cdot H_2O$, 54788-69-1.

**Supplementary Material Available.** A listing of structure factor amplitudes will appear following these pages in the microfilm edition of this volume of the journal. Photocopies of the supplementary material from this paper only or microfiche (105 × 148 mm, 24× reduction, negatives) containing all of the supplementary material for the papers in this issue may be obtained from the Journals Department, American Chemical Society, 1155 16th St., N.W., Washington, D.C. 20036. Remit check or money order for $4.50 for photocopy or $2.50 for microfiche, referring to code number AIC408446.

## References and Notes

(1) L. G. Marzilli, J. G. Salerno, and L. A. Epps, *Inorg. Chem.*, **11**, 2050 (1972).
(2) M. M. Jones, "Ligand Reactivity and Catalysis", Academic Press, New York, N.Y., 1968, p 26.
(3) G. L. Eichhorn in "Inorganic Biochemistry", G. L. Eichhorn, Ed., Elsevier, Amsterdam, 1973, Chapter 33.
(4) L. G. Marzilli, T. J. Kistenmacher, and C. H. Chang, *J. Am. Chem. Soc.*, **95**, 7507 (1973); T. J. Kistenmacher, *Acta Crystallogr., Sect. B*, **31**, 86 (1975).
(5) L. G. Marzilli, T. J. Kistenmacher, P. E. Darcy, D. J. Szalda, and M. Beer, *J. Am. Chem. Soc.*, **96**, 4684 (1974); T. J. Kistenmacher and D. J. Szalda, *Acta Crystallogr., Sect. B*, **31**, 90 (1975).
(6) E. Sletten, *Chem. Commun.*, 558 (1971); *Acta Crystallogr., Sect. B*, **30**, 1961 (1974).
(7) L. Sacconi and I. Bertini, *Inorg. Chem.*, **5**, 1520 (1966).
(8) D. F. Evans, *J. Chem. Soc.*, 2003 (1959).
(9) R. H. Holm and G. W. Everett, *Prog. Inorg. Chem.*, 7, 83 (1966).
(10) W. R. Busing and H. A. Levy, *J. Chem. Phys.*, **26**, 563 (1957).
(11) A. J. C. Wilson, *Nature (London)*, **150**, 152 (1942).
(12) H. P. Hanson, F. Herman, J. D. Lea, and S. Skillman, *Acta Crystallogr.*, **17**, 1040 (1964).
(13) R. F. Stewart, E. R. Davidson, and W. T. Simpson, *J. Chem. Phys.*, **42**, 3175 (1965).
(14) D. T. Cromer, *Acta Crystallogr.*, **18**, 17 (1965).
(15) Supplementary material.
(16) J. M. Stewart, "X-Ray 67", Technical Report 67-58, Computer Science Center, University of Maryland, 1967.
(17) W. R. Busing, K. O. Martin, and H. A. Levy, "ORFLS", Report ORNL-TM-305, Oak Ridge National Laboratory, Oak Ridge, Tenn., 1962.
(18) M. E. Pippy and F. R. Ahmed, "NRC Crystallographic Programs", National Research Council, Ottawa, 1968.
(19) C. K. Johnson, "ORTEP", Report ORNL-3794, Oak Ridge National Laboratory, Oak Ridge, Tenn., 1965.
(20) W. C. Hamilton and J. A. Ibers, "Hydrogen Bonding in Solids", W. A. Benjamin, New York, N.Y., 1968.
(21) T. J. Kistenmacher, L. G. Marzilli, and C. H. Chang, *J. Am. Chem. Soc.*, **95**, 5817 (1973); T. J. Kistenmacher, *Acta Crystallogr., Sect. B*, **30**, 1610 (1974).
(22) L. G. Marzilli, L. A. Epps, T. Sorrell, and T. J. Kistenmacher, *J. Am. Chem. Soc.*, in press.
(23) H. I. Heitner, S. J. Lippard, and H. R. Sunshine, *J. Am. Chem. Soc.*, **94**, 8936 (1972); H. I. Heitner and S. J. Lippard, *Inorg. Chem.*, **13**, 815 (1974).
(24) D. J. Szalda, L. G. Marzilli, and T. J. Kistenmacher, *Biochem. Biophys. Res. Commun.*, **63**, 601 (1975); T. J. Kistenmacher, D. J. Szalda, and L. G. Marzilli, submitted for publication in *Acta Crystallogr.*
(25) M. Sundaralingam and J. A. Carrabine, *J. Mol. Biol.*, **61**, 287 (1971).
(26) K. Saito, R. Terashima, T. Sakaki, and K. Tomita, *Biochem. Biophys. Res. Commun.*, **61**, 83 (1974).
(27) B. J. Hathaway, *Struct. Bonding (Berlin)*, **14**, 49 (1973).
(28) S. C. Yang and P. W. R. Corfield, Abstracts, American Crystallographic Association Meeting, University of Connecticut, Storrs, Conn., June 1973, No. M8.
(29) C. E. Bugg, J. M. Thomas, M. Sundaralingam, and S. T. Rao, *Biopolymers*, **10**, 175 (1971).
(30) B. Pullman, Ed., "Molecular Associations in Biology", Academic Press, New York, N.Y., 1968.
(31) L. S. Lerman, *J. Mol. Biol.*, **3**, 18 (1961).
(32) H. M. Sobell and S. C. Jain, *J. Mol. Biol.*, **68**, 21 (1972).
(33) W. J. Pigram, W. Fuller, and L. D. Hamilton, *Nature (London), New Biol.*, **235**, 17 (1972).
(34) R. L. O'Brien, J. L. Allison, and F. E. Hahn, *Biochim. Biophys. Acta*, **129**, 622 (1966).
(35) M. J. Waring, *J. Mol. Biol.*, **54**, 247 (1970).
(36) S. J. Lippard, K. W. Jennette, G. Vassiliades, and W. R. Bauer, paper presented at the 168th National Meeting of the American Chemical Society, Atlantic City, N.J., Sept. 1974.
(37) E. Sletten and B. Thorstensen, *Acta Crystallogr., Sect. B*, **30**, 2438 (1974).
(38) G. A. Barclay and B. F. Hoskins, *J. Chem. Soc.*, 1979 (1965); J. A. Bertrand and J. A. Kelley, *Inorg. Chim. Acta*, **4**, 203 (1970); J. A. Bertrand, J. A. Kelley, and J. L. Breece, *ibid.*, **4**, 247 (1970); J. A. Bertrand and C. E. Kirkwood, *ibid.*, **6**, 248 (1972).
(39) E. C. Lingafelter and R. L. Braun, *J. Am. Chem. Soc.*, **88**, 2951 (1966).
(40) M. Calligaris, G. Nardin, and L. Randaccio, *Coord. Chem. Rev.*, **7**, 385 (1972).
(41) J. Sletten and L. H. Jensen, *Acta Crystallogr., Sect. B*, **25**, 1608 (1969).
(42) D. Voet and A. Rich, *Prog. Nucleic Acid. Res. Mol. Biol.*, **10**, 183 (1970).
(43) K. N. Raymond, P. W. R. Corfield, and J. A. Ibers, *Inorg. Chem.*, **7**, 1362 (1968).

---

Contribution from the Corporate Research Laboratories,
Exxon Research and Engineering Company, Linden, New Jersey 07036

# Structural Studies of the Intercalation Complexes $TiS_2\cdot NH_3$ and $TaS_2\cdot NH_3$

R. R. CHIANELLI,* J. C. SCANLON, M. S. WHITTINGHAM, and F. R. GAMBLE

*Received January 23, 1975* AIC500610

Crystal structures of the intercalation complexes $TiS_2\cdot NH_3$ and $TaS_2\cdot NH_3$ from X-ray powder intensity data are reported. In $TiS_2\cdot NH_3$, nitrogen is on the midplane between layers in a trigonal-prismatic sulfur environment. The nitrogen cannot be located in $TaS_2\cdot NH_3$. $TiS_2\cdot NH_3$ is rhombohedral with three layers per (hexagonal) unit cell; $TaS_2\cdot NH_3$ is hexagonal with two layers per unit cell. The respective lattice constants are $a = 3.427$ (2) and $c = 26.55$ (2) Å and $a = 3.320$ (5) and $c = 18.16$ (2) Å. Twinning or stacking faults were found to be important.

## Introduction

In 1969 Ruthardt and Weiss[1] reported intercalation complexes between $TiS_2$ and both aliphatic amides and aqueous hydrazine. Gamble and coworkers[2] subsequently showed that the intercalation reaction is quite general. A large class of these compounds is formed between layered disulfides and diselenides of 4B and 5B transition metal and molecular Lewis bases, both organic and inorganic. These new complexes are interesting because of their remarkably anisotropic electron-transport properties[3] and the unusual superconducting properties of the niobium and tantalum dichalcogenide compounds.[4] These electronic properties can be changed systematically by modifying of the electronic and geometrical characteristics of the molecular intercalate. Therefore, the nature of the interaction or chemical bond between intercalate and chalcogenide layer is important. Progress has been

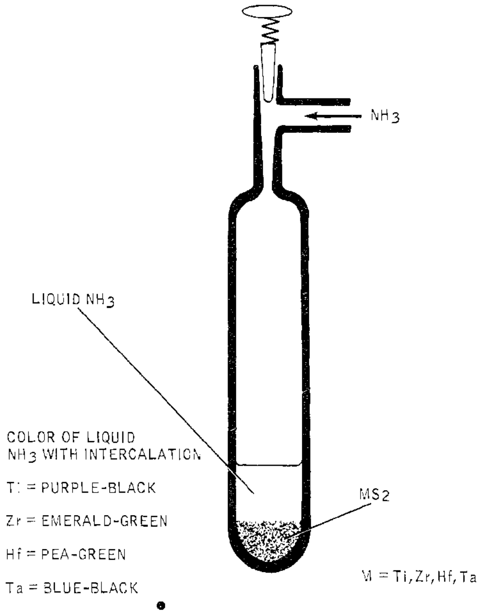

**Figure 1.** Fischer-Porter tube for intercalation of layered dichalcogenides with $NH_3$.

hampered by lack of structural information beyond that inferred from the expansion of the *c* axis on intercalation. We selected $TiS_2{\cdot}NH_3$ and $TaS_2{\cdot}NH_3$ as prototypes for detailed investigation because of the ammonia molecule simplicity and the unusual structural implications of recent NMR studies on $TaS_2{\cdot}NH_3$. Silbernagel and Gamble[5] observed an anisotropic proton spin–lattice relaxation time in single crystals of $TaS_2{\cdot}NH_3$. This indicates that the molecular symmetry axis and, hence, the lone-pair orbital lie parallel to the $TaS_2$ layers, not perpendicular as previously postulated[6] on the basis of traditional chemical arguments. The parallel orientation suggests that nitrogen should lie on the plane midway between disulfide layers. Our results are consistent with this orientation.

The $NH_3$ intercalation complexes of $TiS_2$, $ZrS_2$, $NbS_2$, and $TaS_2$ have been prepared[2] from gaseous and liquid $NH_3$. The aqueous $NH_3$ compounds[2,7] have been shown to be hydrates typified by the formula $(NH_3)_{1/3}(H_2O)_{2/3}TaS_2$.[8] $NH_3$ can also be intercalated by the electrolysis of ammonium salts at a dichalcogenide electrode.[9] In every case, the volume of the sulfide increases 50% and the interlayer distance ($c/n$, where $n$ is the number of layers in the unit cell) increases approximately 3 Å. Under anhydrous conditions with excess $NH_3$, 1 mol of $NH_3$ is intercalated per formula unit of the dichalcogenide. Second- and fourth-stage complexes, where $NH_3$ is between every second or fourth layer, are also known.[2,10] X-Ray diffraction studies of first-stage $NH_3$ compounds have been reported.[6,7] Cousseau et al.[6] found $NH_3$ to be in trigonal-prismatic sites in $ZrS_2{\cdot}NH_3$. Schollhorn and Weiss[7] mentioned a one-dimensional fourier synthesis along 001 for $NbS_2{\cdot}NH_3$, with a peak midway between layers but with "satellites" nearer the layers. In neither case was a structural refinement attempted.

## Sample Preparation

The transition metal disulfides were prepared from the elements by direct combination or vapor transport.[3] They were analyzed chemically and X-ray diffractionally. The highly crystalline products were ground in liquid $N_2$ and sieved through a 325-mesh screen to reduce particle-size effects on X-ray intensities. Grinding did not affect diffraction line widths.

The ground powders were then placed in a tube (Figure 1) with a Fischer–Porter valve designed to withstand 25 atm of pressure. The tube, which had been dried and evacuated, was again evacuated after filling with the disulfide. Liquid $NH_3$ was then condensed in the tube until the powder was covered with a large excess, the valve was closed, and the tube was allowed to come to room temperature.

**Table I.** $TaS_2{\cdot}NH_3$ Powder Diffraction Data ($a = 3.320$ (5), $b = 18.16$ (2) Å)

| *hkl* | $d_{obsd}$, Å | $d_{calcd}$, Å | Calcd $I/I_0$ |
|---|---|---|---|
| 022 | 9.02 | 9.08 | 100 |
| 044 | 4.49 | 4.54 | 13 |
| 006 | 3.03 | 3.00 | 2 |
| 100 | 2.878 | 2.875 | <1 |
| 101 | 2.839 | 2.840 | 25 |
| 102 | 2.739 | 2.741 | 2 |
| 103 | 2.590 | 2.597 | 20 |
| 104 | 2.429 | 2.429 | 12 |
| 105<br>008 | 2.261 | 2.254<br>2.270 | 15 |
| 106 | 2.082 | 2.085 | 9 |
| 107 | 1.929 | 1.926 | 8 |
| 0,0,10 | 1.810 | 1.816 | 2 |
| 108 | 1.785 | 1.782 | 3 |
| 110 | 1.661 | 1.660 | 6 |
| 112 | 1.635 | 1.633 | 7 |
| 114 | 1.559 | 1.559 | 3 |
| 0,0,12 | 1.511 | 1.513 | 1 |
| 116 | 1.458 | 1.455 | 1 |
| 201 | 1.434 | 1.433 | 2 |
| 203 | 1.403 | 1.399 | 2 |
| 204 | 1.372 | 1.370 | 1 |
| 118<br>1,0,12 | 1.340 | 1.340<br>1.339 | 2 |
| 206<br>0,0,14 | 1.298 | 1.299<br>1.297 | 2 |
| 1,1,10 | 1.225 | 1.225 | 2 |
| 0,0,14 | 1.183 | 1.182 | <1 |
| 0,0,16 | 1.135 | 1.135 | <1 |
| 1,1,12 | 1.118 | 1.118 | 2 |
| 120 | 1.087 | 1.087 | <1 |
| 214<br>016 | 1.056 | 1.057<br>1.056 | 1 |
| 1,1,14 | 1.022 | 1.002 | |

Intercalation proceeded fairly readily at room temperature. X-Ray diffraction and thermogravimetric analyses showed that 1 day was sufficient to remove any traces of $TiS_2$ or $TaS_2$. We also prepared $NH_3$ intercalation complexes of $ZrS_2$ and $HfS_2$. Both showed small amounts of starting disulfides even after several days in liquid $NH_3$; much longer periods are required for complete intercalation. We did not attempt to refine these structures. Chemical and thermogravimetric analyses showed that $TiS_2$ and $TaS_2$ had taken up 1 mol of $NH_3$/mol of disulfide. All samples for X-ray diffraction measurements were prepared under dry conditions.

Characteristic color changes of the liquid $NH_3$ during intercalation were observed by Thompson[11] for liquid $NH_3$ and other liquid intercalates. He attributed these colors to dissolved sulfur which may form polysulfide species. This dissolved sulfur results from small amounts of excess sulfur in the host lattice which may be removed by repeated intercalations.

Investigation of intercalated single crystals, produced in the same manner as the powders, showed that the crystals had also undergone a color change. Normally metallic-gold $TiS_2$ turned bronze and $TaS_2$ turned from silver-black to blue-black. $HfS_2$ and $ZrS_2$, which are normally red-orange, turned to darker, bronze-tinged shades of the same color.

We were able to follow the intercalation of single crystals using an optical gas cell with time under the polarizing reflected-light microscope, where severe cracking of the crystals and striking color changes were noted.[12]

## Lattice Parameter Refinements

Powder diffraction patterns were obtained with Cu K$\alpha$ radiation and a Philips diffractometer, calibrated with a quartz standard. All lines were recorded up to $2\theta = 130°$ at a speed of $^1/_4°$ min$^{-1}$. $TaS_2{\cdot}NH_3$ gave lines up to about $2\theta = 100°$, but the lines were somewhat broadened and no $\alpha_1$–$\alpha_2$ doublets could be resolved.

Both patterns were indexed on hexagonal cells and least-squares refinements were done on observed $d$ values greater than $2\theta = 30°$. $TaS_2{\cdot}NH_3$ refined to $a = 3.320$ (5) and $c = 18.16$ (2) Å. $TiS_2{\cdot}NH_3$ gave $a = 3.427$ (2) and $c = 26.55$ (2) Å. The observed and calculated $d$ values are shown in Tables I and II, together with the intensity calculated from the structures discussed in a later section. Only

**Table II.** $TiS_2 \cdot NH_3$ Powder Diffraction Data ($a = 3.427$ (2), $b = 26.55$ (2) Å)

| *hkl* | $d_{obsd}$, Å | $d_{calcd}$, Å | Calcd $I/I_0$ |
|---|---|---|---|
| 003 | 8.91 | 8.85 | 100 |
| 006 | 4.46 | 4.42 | 6 |
| 101<br>009 | 2.964 | 2.967<br>2.949 | 4 |
| 012 | 2.898 | 2.896 | 15 |
| 104 | 2.708 | 2.709 | 1 |
| 015 | 2.594 | 2.590 | 35 |
| 107 | 2.342 | 2.337 | 3 |
| 0,0,12<br>018 | 2.215 | 2.212<br>2.212 | 13 |
| 1,0,10 | 1.981 | 1.978 | 5 |
| 0,1,11 | 1.874 | 1.872 | 3 |
| 0,0,15 | 1.773 | 1.770 | 1 |
| 110 | 1.713 $d\alpha_1$<br>1.713 $d\alpha_2$ | 1.713 | 13 |
| 113<br>$11\bar{3}$<br>1,0,13 | 1.681 | 1.682<br>1.682<br>1.682 | 17 |
| 0,0,18<br>202 | 1.475 $d\alpha_1$<br>1.475 $d\alpha_2$ | 1.475<br>1.475 | 4 |
| 205 | 1.429 | 1.429 | 5 |
| 027 | 1.371 | 1.382 | 1 |
| 0,2,10 | 1.294 | 1.295 | 1 |
| 2,0,11 | 1.262 | 1.264 | 1 |
| 122<br>$21\bar{2}$<br>1,1,18<br>$1,1,\overline{18}$<br>1,0,22 | 1.117 | 1.118<br>1.118<br>1.118<br>1.118<br>1.118 | 5 |
| 125<br>$21\bar{5}$ | 1.097 | 1.097<br>1.097 | 3 |
| $21\bar{8}$<br>128 | 1.062 | 1.063<br>1.063 | 2 |
| 300 | 0.9892 $d\alpha_1$<br>0.9891 $d\alpha_2$ | 0.9892 | 2 |
| $1,2,\overline{13}$<br>2,1,13 | 0.9831 $d\alpha_1$<br>0.9830 $d\alpha_2$ | 0.9831<br>0.9831 | 2 |

calculated intensities are reported because of the wide variation of observed intensities, presumably due to preferred orientation and extinction.

Moisture was found to cause splitting of the 00*l* lines for both $TiS_2 \cdot NH_3$ and $TaS_2 \cdot NH_3$, as previously observed in $NbS_2 \cdot NH_3$.[7] This splitting was variable and could go through several steps; no attempt was made to follow it quantitatively. These additional phases are almost certainly the same type as those formed in hydroxide solutions; thus $(NH_3)_{1/3}(H_2O)_{2/3}TaS_2$ has a $c/n$ of 9.11 Å[2,8] compared to the 9.08 Å found here for $TaS_2 \cdot NH_3$. In addition, insufficient $NH_3$ or reaction time caused extra diffraction lines which would be assigned to higher staged compounds.[2,10] Care was thus taken to avoid these effects by operating under very dry conditions with excess $NH_3$ and allowing sufficient time for complete intercalation; no additional lines or 00*l* splitting was noted in our X-ray patterns.

## Structure

$TiS_2$ has a one-layer trigonal structure (1T) where the metal atom resides in an octahedron of sulfur atoms, while $TaS_2$ has a two-block structure (2H) where the metal atom resides in a trigonal prism of sulfur atoms. On intercalation, the lattice expands perpendicular to the van der Waals layer; in addition the layers can undergo a change in stacking sequence.

Parry et al.[13] have shown from powder X-ray and electron diffraction data that when $TaS_2$ is intercalated with pyridine, the structure goes from 2H where the metal atoms lie above each other to 2H where the sulfur atoms lie above each other. This means that intercalated $NH_3$ groups reside, in a trigonal prism of sulfur, as shown schematically for $TaS_2 \cdot NH_3$ in Figure 2. $TaS_2$ belongs to space group *P*6₃/*mmc* (186) and the intercalated species may be fit into the same space group, if one disregards the $NH_3$ molecule. Parry assigns the complex $TaS_2 \cdot {}^1/_2py$ to this space group. However, this awaits confirmation from X-ray single-crystal measurements.

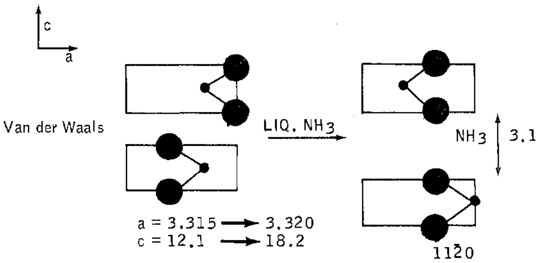

**Figure 2.** Schematic $11\bar{2}0$ representation of the expansion of $TaS_2$ lattice upon intercalation with $NH_3$.

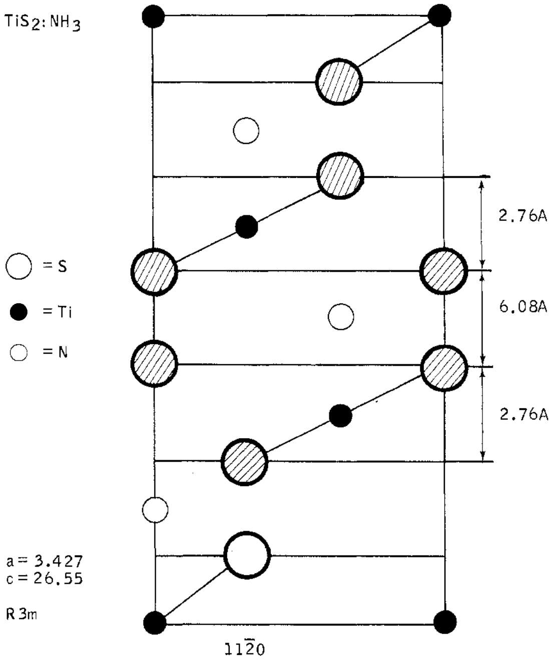

**Figure 3.** The $11\bar{2}0$ section of the $TiS_2 \cdot NH_3$ unit cell.

Cousseau[6] has shown that $ZrS_2 \cdot NH_3$ forms a rhombohedral three-layer structure (3R) isostructural with $KTiS_2$. He assigned $ZrS_2 \cdot NH_3$ on the basis of X-ray powder data to space group *R*3*m* (196) but made no attempt to execute a quantitative crystal structure. $ZrS_2$ goes from a 1T to a 3R structure with intercalation. Figure 3 shows a schematic $11\bar{2}0$ section of this 3R structure for $TiS_2 \cdot NH_3$.

We have attempted to refine the crystal structures of $TaS_2 \cdot NH_3$ and $TiS_2 \cdot NH_3$ with X-ray powder diffraction data, using a refinement program based on the "Simplex" method.[14] The program also handles partial contributions from overlapping reflections. Residuals were calculated on the basis of intensities, i.e.

$$R_I = \Sigma(|I_o| - |I_c|)/\Sigma|I_o|$$

It can be shown that this is approximately equivalent to $2R_F$ where

$$R_F = \Sigma(|F_o| - |F_c|)/\Sigma|F_o|$$

Reported observed intensities were an average of two runs. Refinement of atomic positions used equally weighted cell reflections, isotropic Hartree–Fock calculated scattering factors ($Ti^{4+}$, $Ta^{5+}$, $S^{2-}$, and $N^0$),[15] and corrections for anomalous dispersion (real and imaginary parts).[16]

**$TaS_2 \cdot NH_3$.** Intensity data were recorded with a diffractometer and photographed with a Debye–Scherrer camera. Nickel-filtered Cu K$\alpha$ ($\lambda$ 1.5418 Å) radiation was used in both cases. The photographic intensities were measured by means of a Joyce–Loebl densitometer. Obtaining good intensity data with the heavily absorbing tantalum atoms present was difficult. The diffractometer data were difficult to reproduce,

**Table III.** $TaS_2 \cdot NH_3$ ($R_I = 20.8\%$) Diffractometer Data

| | $I/I_0$ | | | $I/I_0$ | |
|---|---|---|---|---|---|
| *hkl* | Obsd | Calcd | *hkl* | Obsd | Calcd |
| 002 | 90 | 96 | 0,0,10 | 4.0 | 1.8 |
| 004 | 22 | 11 | 108 | 4.0 | 2.2 |
| 006 | 4.0 | 1.5 | 110 | 3.0 | 8.6 |
| 101 | 26 | 22 | 109 | | |
| 102 | 2.0 | 2.1 | 112 | | |
| 103 | 13 | 17 | 1,0,10 | 0.1 | 0.1 |
| 104 | 9.0 | 12 | 1,0,11 | 2.0 | 3.9 |
| 105 | 14 | 14 | 200 | | |
| 008 | | | 201 | | |
| 106 | 8.0 | 8.0 | 202 | | |
| 107 | 6.0 | 6.2 | 1,0,12 | 0.1 | 0.1 |

**Table IV.** $TaS_2 \cdot NH_3$ Atomic Positions[a]

| *x* | *y* | *z* |
|---|---|---|
| | Tantalum | |
| 0 | 0 | $^1/_4$ |
| $^2/_3$ | $^1/_3$ | $^3/_4$ |
| | Sulfur | |
| $^1/_3$ | $^2/_3$ | 0.1630 (5) |
| $^1/_3$ | $^2/_3$ | 0.3370 (5) |
| $^1/_3$ | $^2/_3$ | −0.3370 (5) |
| $^1/_3$ | $^2/_3$ | −0.1630 (5) |
| | Nitrogen (Proposed) | |
| $^2/_3$ | $^1/_3$ | 0 |
| 0 | 0 | $^1/_2$ |

[a] Interatomic distances: interlayer S–S distance, 5.93 (1) Å; intralayer S–S distance, 3.17 (1) Å; Ta–S bond distance, 2.49 (2) Å; intralayer S–S distance perpendicular to *c*, 3.320 (5) Å.

especially the 00*l* series. We attribute this to preferred orientation of the platelike crystals and to extinction effects. However, several runs of carefully ground and sieved samples (as previously described) yielded good reproducibility.

The powder photographs confirmed the preferred orientation problem and here the strong lower angle lines were discarded in the refinement. Absorption corrections were made to the measured powder intensities. For Cu radiation using a 0.03-cm diameter capillary tube, $\mu r$ was greater than 20. For Cu the linear absorption coefficient is 693 cm$^{-1}$ and for Mo it is 346 cm$^{-1}$ with $TaS_2 \cdot NH_3$, which has a calculated density of 5.06 g/cm$^3$.

The loss of information due to overlapping peaks was much greater for Mo than for Cu; since the tantalum is still heavily absorbing, nothing is gained by switching to Mo. Powder photographs removed some but not all of the preferred orientation effects. Table III gives the observed and calculated diffractometer data.

The best agreement between observed and calculated data is obtained with the structure shown schematically in Figure 4. The atomic positions are listed in Table IV. All positions except the sulfur *z* parameters were fixed. The diffractometer data gave the lower residual, $R_I = 20.8\%$. However, both refinements gave the same sulfur *z* parameter. Although the residuals are quite high, no other structures gave residuals lower than $R_I = 60\%$. The high residuals are attributed to poor data due to high absorption preferred orientation and probably the disorder in the crystals discussed later. No improvement is likely with only X-ray powder data. Refinement was completely insensitive to the $NH_3$ position. However, neutron diffraction data are currently under evaluation at Argonne National Laboratory in hopes of determining the position of the $NH_3$ molecule in $TaS_2 \cdot NH_3$.[17]

Atomic positions for the Ta and S atoms in Table IV are the same as those reported for $TaS_2 \cdot py$ by Parry et al.[13]

**$TiS_2 \cdot NH_3$.** For $TiS_2 \cdot NH_3$, Mo radiation greatly reduces adsorption effects. The linear absorption coefficient is 33.5 cm$^{-1}$ and $\mu r$ is 1.01 for a 0.03-cm diameter capillary. Debye–Scherrer films were free from preferred orientation effects. The intensities were measured with a Joyce–Loebl densitometer and the absorption corrections were applied for the 0.03-cm diameter capillary ($\mu r = 1.00$).

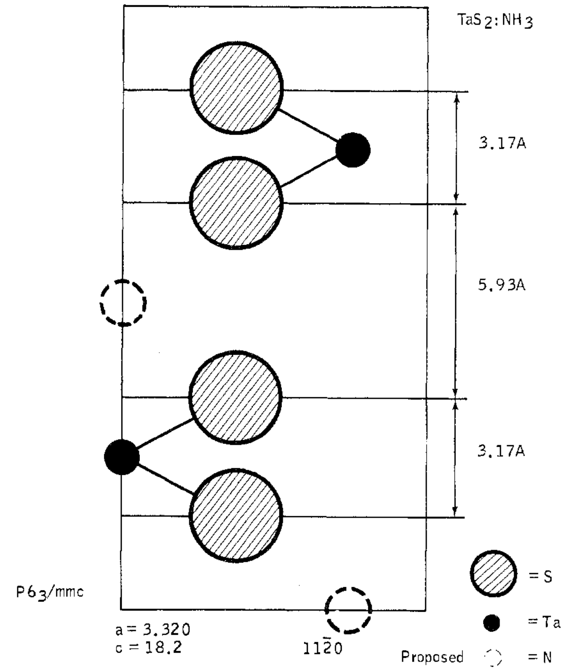

Figure 4. The 11$\bar{2}$0 section of the $TaS_2 \cdot NH_3$ unit cell.

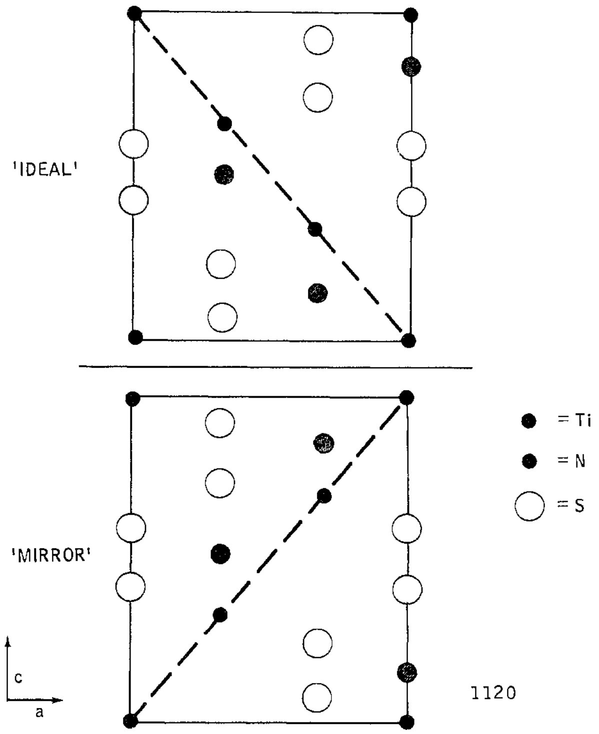

Figure 5. Schematic representation of the "twinning" operation in $TiS_2 \cdot NH_3$.

The structure was calculated initially using the atomic positions of Figure 3. Refinement of the *z* parameters dropped the residual to $R_I = 20.4\%$. Since it was felt that the data were better than this high residual would suggest, we assumed that some disorder was present.

Schollhorn and Weiss[7] reported two-dimensional disorder in $NbS_2 \cdot NH_3$ as revealed by single-crystal photographs. The 101 and 201 or, in general, the *hkl* reflections were linked by blackening which did not appear when *h* or *k* = 3. This they

**Table V.** $TiS_2 \cdot NH_3$ Atomic Positions ("Mixed Crystal")[a]

| | $x$ | $y$ | $z$ | Isotropic temp factor | Occupancy |
|---|---|---|---|---|---|
| | | | Titanium | | |
| "Ideal" | 0 | 0 | 0 | 0.167 | 1.00 |
| | 1/3 | 2/3 | 2/3 | 0.167 | 0.69 |
| | 2/3 | 1/3 | 1/3 | 0.167 | 0.69 |
| "Mirror" | 1/3 | 2/3 | 1/3 | 3.045 | 0.28 |
| | 2/3 | 1/3 | 2/3 | 3.045 | 0.28 |
| | | | Sulfur | | |
| "Ideal" | 0 | 0 | 0.6147 (5) | 0.133 | 1.00 |
| | 0 | 0 | 0.3853 (5) | 0.133 | 1.00 |
| | 2/3 | 1/3 | 0.9480 (5) | 0.133 | 0.69 |
| | 2/3 | 1/3 | 0.7187 (5) | 0.133 | 0.69 |
| | 1/3 | 2/3 | 0.0520 (5) | 0.133 | 0.69 |
| | 1/3 | 2/3 | 0.2813 (5) | 0.133 | 0.69 |
| "Mirror" | 1/3 | 2/3 | 0.9480 (5) | 1.780 | 0.28 |
| | 1/3 | 2/3 | 0.7187 (5) | 1.780 | 0.28 |
| | 2/3 | 1/3 | 0.2813 (5) | 1.780 | 0.28 |
| | 2/3 | 1/3 | 0.0520 (5) | 1.780 | 0.28 |
| | | | Nitrogen | | |
| "Ideal" | 2/3 | 1/3 | 1/2 | 0.291 | 1.00 |
| | 0 | 0 | 0.167 | 0.291 | 0.69 |
| | 1/3 | 2/3 | −0.167 | 0.291 | 0.69 |
| "Mirror" | 0 | 0 | −0.167 | 1.356 | 0.28 |
| | 1/2 | 2/3 | 0.167 | 1.356 | 0.28 |

[a] $R_I = 9.6\%$; λ(Mo Kα) 0.7110 Å; overall cell temperature parameter 1.195. Interatomic distances: interlayer S–S distance, 6.09 (1) Å; S–Ti–S layer distance parallel to the $c$ axis, 2.76 (1) Å; Ti–S bond distance, 2.41 (2) Å; interlayer S–S distance parallel to the $a$ axis, 3.427 (2) Å; intralayer S–S distance, 3.40 (2) Å.

interpreted as statistical displacement of $NH_3$ intercalation layers by $a/3$ or $b/3$.

In addition Bartram[18] reported that crystals of $TiS_2$ were twinned along 00$l$ planes, from single-crystal photographs. He found that this twinning which mirrors the atoms across 00$l$ planes, occurred randomly with 70% of the atoms in "ideal" sites and 30% in the "mirror" or twinned sites.

We felt that if this type of disorder was present in the starting material, it would also be present in the intercalated materials. Calculations showed that for space group $R\bar{3}m$ (as for the original $TiS_2$ space group $P3m1$), this effect could be observed with powder data. Therefore, the atomic positions were mirrored as is shown in Figure 5, and each position was given an occupancy factor.

Refinement of the occupancy factors of "ideal" and "mirror" atomic positions led to a drop in the residual to $R_I = 9.5\%$. The occupancy factors refined to roughly 0.69 "ideal" and 0.28 "mirror". Atomic positions and occupancy factors are shown in Table V, and final intensity data are shown in Table VI. We, therefore, conclude that this type of "twinning" is present in $TiS_2 \cdot NH_3$ and probably reflects original "twinning" in the $TiS_2$ starting material. The sulfur $z$ parameters were again refined after the introduction of the twinning with no significant change.

The intensity data are sensitive to the N position and all models which removed it from the center of the trigonal prism on the plane halfway between sulfurs led to significantly higher residuals, both before and after the refinement due to "twinning". Such models included splitting N off the center plane of the trigonal pyramid. The low residual makes further refinement unlikely to yield new information.

## Discussion

The basic structure of $TaS_2 \cdot NH_3$ and $TiS_2 \cdot NH_3$ has been described. In both cases, the $NH_3$ molecule lies in a trigonal prism of sulfur. The height of this trigonal prism is 6.09 (1) Å for $TiS_2 \cdot NH_3$ and 5.93 (1) Å for $TaS_2 \cdot NH_3$. The difference is probably due to the different coordination about the metal atoms and to the greater covalency of the Ta–S bond. The M–S bond distances reported are about the same as those estimated for the nonintercalated materials (Ti–S = 2.42 Å and Ta–S = 2.48 Å).[19] The octahedron of S atoms around Ti in $TiS_2 \cdot NH_3$ is slightly distorted. The S–S distance is 3.43 Å within the S triangles but 3.40 Å between S atoms in different triangles. This difference means that the $TiS_6$ octahedron has a negative trigonal distortion and the S–Ti–S layers are slightly flattened, compared to the structure where the S atoms are in a perfect octahedron around the titanium.

**Table VI.** $TiS_2 \cdot NH_3$ Intensity Data [λ(Mo Kα) 0.7110 Å]

| | $I/I_0$ | | | $I/I_0$ | |
|---|---|---|---|---|---|
| $hkl$ | Obsd | Calcd | $hkl$ | Obsd | Calcd |
| 101<br>009<br>012 | 50 | 48 | 1,1,15<br>1,1,$\bar{15}$<br>0,1,20<br>0,2,13 | 12 | 15 |
| 015<br>104 | 133 | 133 | 12$\bar{1}$<br>211<br>122<br>1,1,18<br>1,1,$\bar{18}$ | 19 | 23 |
| 107 | 7.5 | 8.4 | 1,0,22<br>12$\bar{4}$<br>214<br>0,2,16<br>0,0,24<br>125<br>21$\bar{5}$<br>12$\bar{7}$<br>217<br>2,0,17<br>0,1,23 | 30 | 26 |
| 018<br>0,0,12 | 60 | 59 | 21$\bar{8}$<br>128 | | |
| 1,0,10 | 36 | 26 | 1,2,$\bar{10}$<br>2,1,10<br>2,1,$\bar{11}$<br>1,2,11<br>0,2,19<br>1,1,$\bar{21}$<br>1,1,21 | 14 | 14 |
| 0,1,11 | 12 | 11 | 1,0,25<br>300<br>2,0,20<br>033<br>303<br>1,2,$\bar{13}$<br>2,1,13<br>0,0,27 | 17 | 17 |
| 0,0,15 | 2.0 | 3.6 | | | |
| 110<br>113<br>11$\bar{3}$<br>1,0,13 | 138 | 147 | | | |
| 116<br>11$\bar{6}$<br>0,1,14 | 9.0 | 7.7 | | | |
| 027<br>119<br>11$\bar{9}$<br>202<br>0,0,18 | 25 | 21 | | | |
| 024<br>1,0,16<br>205 | 18 | 24 | | | |
| 027<br>0,1,17 | 1.0 | 1.5 | | | |
| 208<br>1,1,12<br>1,1,$\bar{12}$ | 14 | 11 | | | |
| 0,2,10 | 8.8 | 5.8 | | | |
| 2,0,11<br>1,0,19<br>0,0,21 | 2.0 | 6.6 | | | |

We have found that "twinning" is important in $TiS_2 \cdot NH_3$, and it is likely that this type of disorder is common in the layered transition metal chalcogenides. Polytypism is well known in $CdI_2$, the prototype for 1T type layered chalcogenides. The mechanism of this "twinning" is unknown. The twinning could be also properly described as stacking faults. Figure 5 probably does not represent the actual disorder present in the crystal, but only statistical atomic positions. However, in view of Bartram's[18] description of $TiS_2$, it seems likely that the twinning observed in $TiS_2 \cdot NH_3$ was inherent in nonintercalated $TiS_2$. Therefore, we are undertaking X-ray single-crystal and electron microscopic studies to determine the exact nature of the "twinning" in these compounds. The 00$l$ "twinning" described by Bartram is equivalent to a 60° rotation of a layer with respect to another layer. It is also quite likely that similar disorder is present in $TaS_2 \cdot NH_3$, although it would not be revealed in powder data because of symmetry conditions. Note that 2H $TaS_2$ is obtained by slow cooling the reaction product of the elements at 900°. It is known that 1T $TaS_2$ is formed initially and then transforms at lower temperatures to 2H.[20] This transition may cause considerable disorder which is retained in 2H $TaS_2 \cdot NH_3$. Also, in $TaS_2$

both before and after intercalation, the *h0l* series shows alternately sharp and broad lines (sharp when $l = 2n$) which can be attributed to this type of disorder. Finally, Jellinek has reported that stacking faults frequently occur in $TaS_2$.[21] Nevertheless, the disorder must be understood more fully before precise structural information about the intercalated molecules can be obtained.

Our studies of $TiS_2 \cdot NH_3$ were undertaken to determine the position of the N atom of the intercalated $NH_3$ molecule. We have found a best fit by placing N on the midplane between the layers in the center of the trigonal prism. This position was predicted by Silbernagel and Gamble[5] from their studies of the anisotropy of the proton spin–lattice relaxation time in single crystals of $TaS_2 \cdot NH_3$, which indicate the molecular threefold symmetry axis is parallel to the layers. This suggests that the N should reside at the midplane. From our data, no strong inference can be drawn regarding the $NH_3$ orientation, but the midplane location of the nitrogen is firmly established for $TiS_2 \cdot NH_3$.

**Acknowledgment.** We thank J. M. Longo for his assistance in setting up the atomic parameter refinement program. We also thank M. B. Dines, B. G. Silbernagel, and A. H. Thompson for their helpful discussions and advice.

**Registry No.** $TiS_2 \cdot NH_3$, 34303-30-5; $TaS_2 \cdot NH_3$, 34340-90-4.

## References and Notes

(1) A. Weiss and R. Ruthhardt, *Z. Naturforsch., Teil B*, **24**, 355 (1969).
(2) F. R. Gamble, J. H. Osiecki, M. Cais, R. Pisharody, F. J. DiSalvo, and T. H. Geballe, *Science*, **174**, 493 (1971).
(3) F. R. Gamble and T. H. Geballe, *Treatise Solid State Chem.*, **3** (1975).
(4) F. R. Gamble, F. J. DiSalvo, R. A. Klemm, and T. H. Geballe, *Science*, **168**, 568 (1970).
(5) B. G. Silbernagel and F. R. Gamble, *J. Chem. Phys.*, in press.
(6) J. Cousseau, L. Trichet, and J. Rouxel, *Bull. Soc. Chim. Fr.*, 872 (1973).
(7) R. Schollhorn and A. Weiss, *Z. Naturforsch., Teil B*, **27**, 1273 (1972).
(8) M. S. Whittingham, *Mater. Res. Bull.*, **9**, 1681 (1974).
(9) M. S. Whittingham, *J. Chem. Soc., Chem. Commun.*, 308 (1974).
(10) M. B. Dines, F. R. Gamble, R. B. Levy, and M. S. Whittingham, Abstracts, 168th National Meeting of the American Chemical Society, Atlantic City, N.J., Sept 10, 1974, No. INOR 47.
(11) A. H. Thompson, *Nature (London)*, **251**, 392 (1974).
(12) R. R. Chianelli, to be submitted for publication.
(13) G. S. Parry, C. B. Scruby, and P. M. Williams, *Philos. Mag.*, **29**, 601 (1974).
(14) J. M. Longo, J. A. Kafalas, and R. J. Arnott, *J. Solid State Chem.*, **3**, 174 (1971).
(15) D. T. Cromer and J. B. Mann, *Acta Crystallogr., Sect. A*, **24**, 321 (1968).
(16) "International Tables for X-Ray Crystallography", Vol. II, Kynoch Press, Birmingham, England, 1968, p 213.
(17) R. R. Chianelli, F. R. Gamble, J. C. Scanlon, and B. G. Silbernagel, Abstracts, 168th National Meeting of the American Chemical Society, Atlantic City, N.J., Sept 10, 1974, No. INOR 48.
(18) S. F. Bartram, Ph.D. Thesis, Rutgers University, 1958.
(19) F. R. Gamble, *J. Solid State Chem.*, **9**, 4, 358 (1974).
(20) F. Jellinek, *Ark. Kemi.*, **20**, 447 (1962).
(21) F. Jellinek, *J. Less-Common Met.*, **4**, 9 (1962).

---

Contribution from the Department of Chemistry,
Kent State University, Kent, Ohio 44242

# Electron Transfer through Organic Structural Units. XX. Reductions at High Ionic Strength[1]

JEAN C. THOMAS, JOHN W. REED, and EDWIN S. GOULD*

*Received October 28, 1974* AIC40745S

The reductions of acetato- and propionatopentaamminecobalt(III) with chromium(II), vanadium(II), and europium(II) (25°, $\mu = 4.0$) are strongly retarded as $(H^+)$ is increased from 0.10 to 4.0 *M*, with the observed dependencies being far too steep to be attributed reasonably to medium effects. The reactions conform to a rate law (eq 2) consistent with partition of the cobalt(III) complex into a nonprotonated and a more slowly reacting protonated form. Acidity constants for the protonated forms of both oxidants have been evaluated, as have the specific rates for the reactions of the two forms of these oxidants with $V^{2+}$ and $Eu^{2+}$. We have been unable to detect the protonated path for reduction of the protonated acetato complex with $Cr^{2+}$, and the specific rate for the protonated propionato derivative is marginal. The nonprotonated reduction paths are predominantly (although not entirely) inner sphere, but the $k_V/k_{Eu}$ ratios calculated for the protonated paths correspond closely to the ratios observed for known outer-sphere series (and differ markedly from inner-sphere ratios). This correspondence confirms the reality of the protonated specific rates and indicates that the protonated path is outer sphere, with the carbonyl oxygen blocked off by protonation. The specific rates for the protonated paths are $10^2$ times those calculated for the (minor) outer-sphere components for the nonprotonated route, this ratio being in accord with the stipulation that electron withdrawal from coordinated Co(III) accelerates outer-sphere reduction of that metal center.

Acetatopentaaminecobalt(III) was one of the original oxidants used to demonstrate electron transfer through an organic ligand.[2] Although an approximate specific rate was reported in 1955 for the reaction of this species with $Cr^{2+}$ in 0.1 *M* $HClO_4$,[2] 16 years elapsed before an acid dependency was established.[3] In 1971, Barrett and coworkers[3a] presented rate data closely following eq 1, an expression consistent with

$$\text{rate} = \frac{k_A(\text{Cr}^{\text{II}})(\text{Co}^{\text{III}})}{1 + (\text{H}^+)/K_{\text{HA}}} \qquad (1)$$

partition of the acetato complex into two forms, an unreactive protonated form (having acidity constant $K_{HA}$) and a reactive nonprotonated form reduced at specific rate $k_A$. This system is of particular interest, for, in contrast to many known acid-dependent Co(III)–Cr(II) reactions,[4] there is a strong likelihood that protonation occurs here at the carbonyl oxygen, tying up the lead-in function[5] and blocking off the inner-sphere path.

Since protonation equilibria involving the oxidant should be independent of the reductant taken, acid dependencies are to be anticipated for other reductions of the acetato complex. In addition, evidence for protonation equilibria would be expected to arise from examination of the reactions of other alkylcarboxylato complexes.

In the present investigation, which pursues these points, many of the measurements have been made at high ionic strength ($\mu = 4.0$), using $LiClO_4$ as the supporting electrolyte. The greater $\mu$ allows experiments embracing a wider range of acidity. Moreover, as has been shown for similar equilibria involving this charge type,[3a,6] these dipositive acids are more completely protonated at greater ionic strengths, bringing into sharper focus the trends we seek. Although our data should perhaps be interpreted with some caution, we feel justified in